Characterization of Magnesium Doped Lithium Iron Silicate

Juan A. Jaén,[1,*] Josefina Iglesias,[2] Alcides Muñoz,[3] Jesús A. Tabares,[4] Germán A. Pérez Alcázar[4]

[1] Departamento de Química Física, CITEN, Edificio de Laboratorios Científicos-VIP, Universidad de Panamá, Panamá

[2] Laboratorio de Análisis Industriales y Ciencias Ambientales, Universidad Tecnológica de Panamá, Panamá

[3] Departamento de Física, Universidad de Panamá, Panamá

[4] Departamento de Física, Universidad del Valle, AA 25360, Cali, Colombia

* Corresponding author's e-mail address: juan.jaen@up.ac.pa

THIS PAPER IS DEDICATED TO DR. SVETOZAR MUSIĆ ON THE OCCASION OF HIS 70TH BIRTHDAY

Abstract: The synthesis of Mg doped $Li_2Fe_{1-x}Mg_xSiO_4$ (x = 0, 0.10 and 0.15) *via* solid-state reaction is reported. The product was characterized by Mössbauer spectroscopy (MS), X-ray diffraction (XRD), Fourier transform infrared spectroscopy (FTIR), magnetic measurements and scanning electron microscopy (SEM). The structures of the reaction products were confirmed to be the monoclinic structure $P2_1/n$, but impurities were detected in them. In the undoped sample small amounts of lithium iron oxide or lithiated magnetite was obtained, whereas a magnetic phase was found in samples with more than 10 % (mole fraction) of Mg doping.

Keywords: lithium iron silicate, cathode material, Mg doping, Mössbauer spectroscopy.

INTRODUCTION

SINCE it was proposed in 2005 by Nytén *et al*.,[1] lithium iron silicate (Li_2FeSiO_4) has drawn considerable attention as one of the most promising cathode materials for lithium-ion batteries. This material is environmentally friendly, made from naturally occurring elements, safe, and has good operating voltage, energy storage capability and high cycling stability. However, it has limited electrical conductivity, and slow Li transport.[2] To overcome these shortcomings numerous alternatives have been proposed, among them doping with an isovalent cation.[3–6]

In recent work, Zhang *et al*.[7] reported the results of the partial substitution of iron by magnesium (up to 3 %, mole fraction) in the monoclinic structure (space group: $P2_1$) using a sol–gel synthesis method, without destroying the structure of the orthosilicate, and improving the electrochemical properties of the Li_2FeSiO_4 cathode materials. Resulting compound, $Li_2Fe_{0.97}Mg_{0.3}SiO_4$, exhibits a better cycle stability and reversibility, than the one from undoped Li_2FeSiO_4. Huang *et al*.[8] also reported

on composites $Li_2Fe_{0.97}Mg_{0.3}SiO_4$ but with the orthorhombic structure indexed to the $Pmn2_1$ space group. Similar good electrochemical properties were reported for uniform nano-sized pure $Li_2Fe_{0.45}Mn_{0.45}Mg_{0.1}SiO_4$ by hydrothermal method followed by carbon coating.[9] Mg doping also has been successfully used in the olivine cathode materials nano-sized $LiFe_{1-x}Mg_xPO_4$–C (x = 0.00, 0.02, 0.04, 0.06 and 0.08).[10] Mg-doped $LiFe_{0.96}Mg_{0.04}PO_4$–C has a remarkable effect on improving the electronic or ionic mobility, but serious electrochemical degradation can occur when its doping density is above 0.04 mol.

In this work, the effect of doping with different Mg mole fractions (0.00–0.15 mol) on the structure of the orthosilicate prepared *via* a solid-state reaction was investigated using X-ray diffraction (XRD), Mössbauer spectroscopy (MS), Fourier transform infrared spectroscopy (FTIR), scanning electron microscopy (SEM), and magnetization measurements. Mössbauer spectroscopy is suitable for providing information on the microscopic structure of iron containing materials.

EXPERIMENTAL SECTION

Lithium metasilicate Li_2SiO_3 (GFS Chemicals, ≥ 99.5 %), di-hydrated iron oxalate $FeC_2O_4 \cdot 2H_2O$ (Aldrich Chemicals, 99 %) and tetrahydrated magnesium acetate $Mg(C_2H_3O_2)_2 \cdot 4H_2O$ (GFS Chemicals, ≥ 99.9 %) were mixed in stoichiometric amounts. Different amounts of magnesium were used in order to obtain 0, 5, 10, and 15 % (mole fraction) of magnesium-doped orthosilicates $Li_2Fe_{1-x}Mg_xSiO_4$. The mixture was ground in a planetary mill, model "Pulverisette 5", for 36 hours, at a frequency of 5 Hz and a vacuum of 2×10^{-5} bar. Then, the dried mixture was pelleted at a pressure of 750 psi (5.17×10^6 Pa) and heated in a horizontal quartz tube oven Hoskins FD303A to 650 °C at 10 °C / min. The process was conducted with an argon flow for a period of 12 hours, after which it was cooled at a rate of –10 °C / min to room temperature.

The crystallographic structural characterization of samples was analyzed by X-ray diffraction (XRD, PANalytical X'Pert powder diffractometer, Cu Kα radiation). All XRD measurements were carried out at room temperature (298 K) in the range of $10° \leq 2\theta \leq 90°$ at intervals of 0.02°, in Bragg-Brentano geometry. The Rietveld refinement of the XRD patterns were made with the GSAS software,[11] based on a Pseudo Voigt profile function (0.75 0.25 Lorentzian and Gaussian). The cell parameters were determined by full-pattern refinement from the XRD data using the GSAS Software. Crystallographic information files (CIF) of Li_2FeSiO_4 were generated from the structural results reported by Mali *et al.*[12] and Sirisopanaporn *et al.*[13]

Mössbauer spectra (MS) were recorded using a conventional spectrometer of constant acceleration with a $^{57}Co(Rh)$ source of activity of 5–10 mCi (185–370 MBq). The measurements were performed at 298 K. The spectra were recorded in transmission geometry. The velocity and isomer shifts were calibrated with an α-Fe foil standard. Spectra were fitted using a standard least-squares fitting routine with Lorentzian lines with the Recoil software (University of Ottawa, Canada).

IR spectra were recorded in transmittance mode using a Shimadzu IR-Affinity-1 (FT-IR 8400S) spectrometer. The resolution of the spectra was 4 cm^{-1}. The spectra obtained were handled with software Academic Know It All.

The morphology of the samples was examined using a JEOL JSM-5600 scanning electron microscope (SEM), equipped with an energy-dispersive X-ray (EDX) detector, and operated at an accelerating voltage of 15 and 20 kV. The magnetization was measured using a Vibrating Sample Magnetometer (VSM) (Quantum Design PPMS VSM P525).

RESULTS AND DISCUSSION

XRD patterns of all samples are shown in Figure 1. A full Rietveld refinement was carried out showing that the dominant crystal phases of all the samples are the monoclinic structure $P2_1/n$. The pristine undoped sample has an extra reflection at 42.87°, as shown in Figure 1e, indicating an impurity, which is attributed to lithium iron (III) oxide.[14] The Mg-doped samples gave patterns similar to those of the undoped Li_2FeSiO_4. No $Li_xFe_2O_3$ is obtained, but a reflection around 44.6° (marked with asterisk in Figure 1 and highlighted with a vertical line in Figure 1e) is particularly observed for samples doped with more than 10 % Mg (mole fraction). In that region, pristine Li_2FeSiO_4 shows some consecutive weak diffraction peaks, but the pattern profiles suggest the contribution of another phase. This reflection matches the (001) characteristic peak of metallic iron, reported as an impurity phase in Li_2FeSiO_4/C material prepared via a solid-state reaction process.[15] Contamination from the extensive milling procedure is excluded, as assessed by weighing the balls before and after each milling. Additional confirmation could be obtained from Mössbauer results discussed later. Very small amounts of other impurities, such as lithium iron (III) catena-disilicate $LiFe(Si_2O_6)$, should not be ruled out in the doped orthosilicates. The most prominent Bragg peaks of this compound occur at 29.842° and 31.295°. A full Rietveld refinement was carried out on the pristine and Mg-doped Li_2FeSiO_4 samples, and the refined lattice parameters are listed in Table 1. The reliability factors R_w are 11.9 %, 11.4 %, 14.2 % and 12.3 % for the undoped and 5, 10 and 15 % (mole fraction) Mg doped, respectively. There is a certain intensity variation in some lines of the diffractogram that may be related to Mg entering the crystal lattice of the orthosilicates provoking changes in the structure, site occupation, or the formation of other phases like $LiFeSiO_4$, a delithiated lithium iron

Table 1. Lattice parameters of $Li_2Fe_{1-x}Mg_xSiO_4$ (x = 0, 0.05, 0.10, 0.15)

| Sample	a / Å	b / Å	c / Å	β / °	V / Å³
X = 0	8.2313	5.0159	8.2331	99.214	335.712
X = 0.05	8.2238	5.0215	8.2407	99.065	336.057
X = 0.10	8.2245	5.0145	8.2339	98.949	335.446
X = 0.15	8.2231	5.0170	8.2449	98.892	336.058
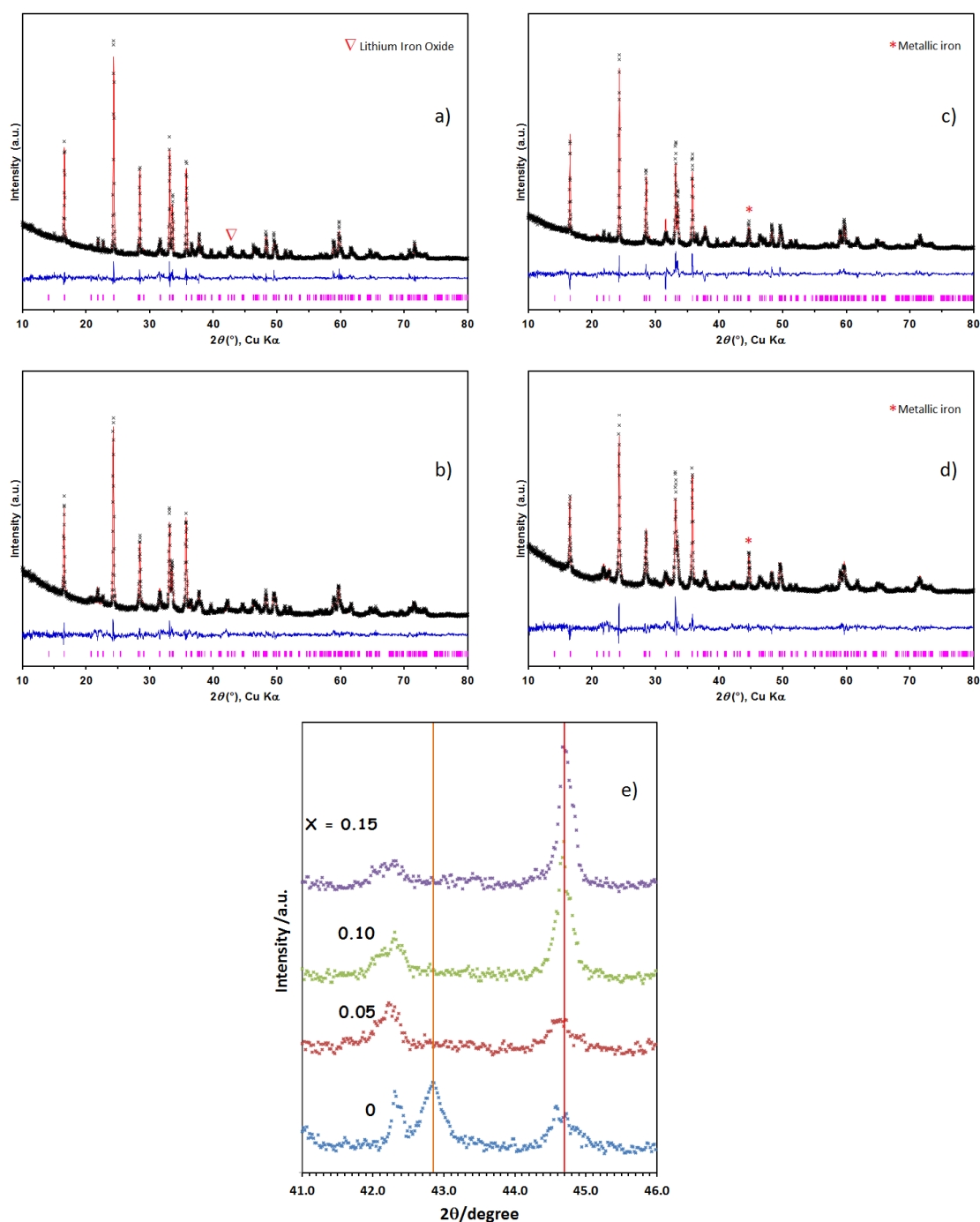
Figure 1. Experimental XRD patterns (*x* marked) compared with the Rietveld-refined profile (solid line) and difference curve of the Mg doped orthosilicates a) *x* = 0 b) *x* = 0.05 c) *x* = 0.10 d) *x* = 0.15. The Bragg positions of the orthorhombic space group *P21/n* are given and impurities are denoted. e) Enlarged zones of XRD patterns displaying peaks from 41° to 46°. The vertical line corresponds to lithium iron (III) oxide[14] (left) and to metallic iron (right).

silicate. Lithium delithiated compound has the same structure as the lithiated silicate with almost the same lattice parameters. The existence of impurities precludes better fittings in Rietveld refinements of XRD data. The lattice parameters and unit cell volume do not give the expected slight decrease after doping with Mg because of the smaller ionic radius in tetrahedral coordination of Mg^{2+} (0.57 Å) compared with that of Fe^{2+} (0.63 Å). In a previous work,[16]

DOI: 10.5562/cca2764

Croat. Chem. Acta **2015**, *88*(4), 487-493
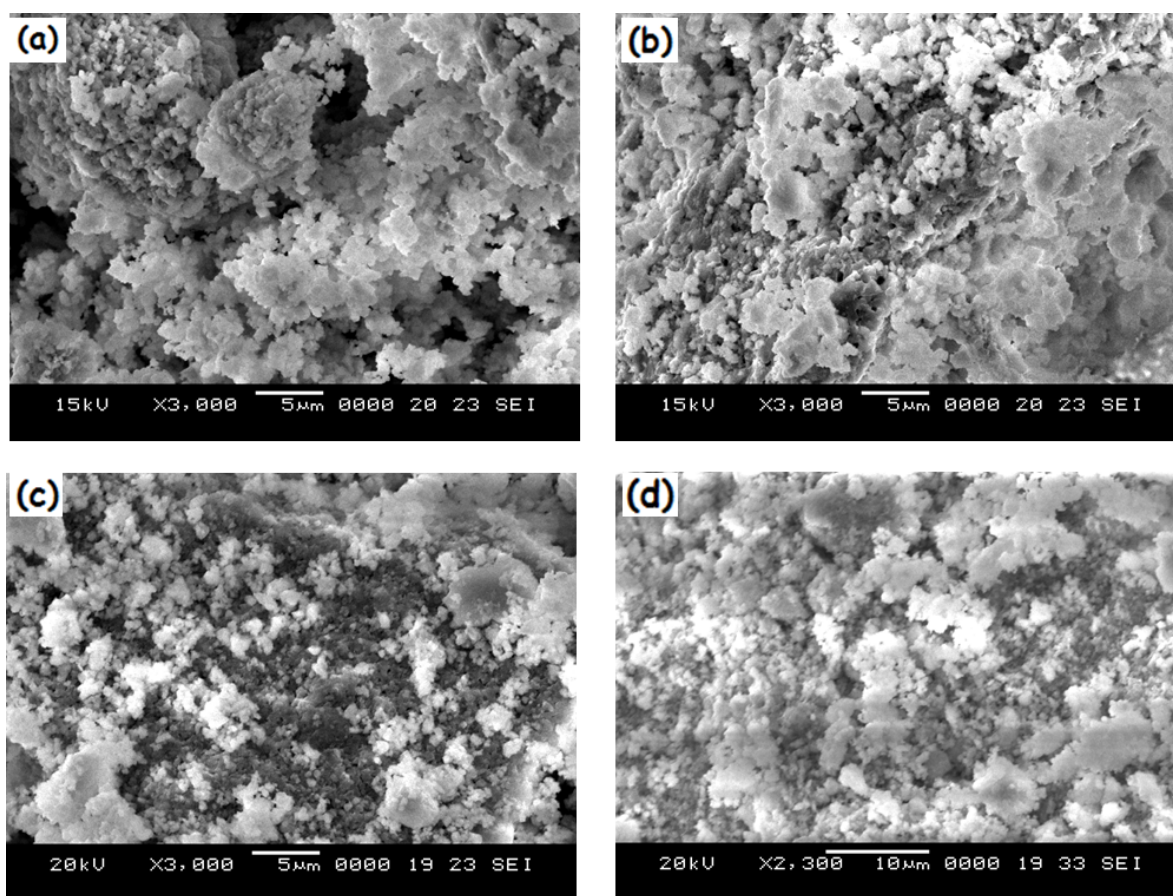
Figure 2. SEM images of $Li_2Fe_{1-x}Mg_xSiO_4$ (a) $x = 0$ (b) $x = 0.05$ (c) $x = 0.10$ (d) $x = 0.15$.

an opposite trend to the one expected using Ni as dopant was observed. It was argued that cation disorder and structural defects introduced during milling process, and delithiation of the orthosilicate, induce lattice expansion. Huang *et al.*[8] proposed that Li ions should have been partially substituted by Mg ions in the orthorhombic polymorph.

Figure 2 shows the SEM images of prepared orthosilicates. As shown, all the samples are composed of agglomerated small sphere-like particles with a broad micrometer-size distribution. Magnesium doping does not make apparent

changes in the morphology, but Mg-doped samples show somewhat less agglomeration. The crystallite size calculated from the Scherrer's equation on the XRD patterns was determined to be 181.9, 119.6, 150.0, and 76.5 nm for the undoped, 5, 10 and 15 % (mole fraction) for Mg doped, respectively.

Mössbauer spectroscopy measurements at room temperature of all samples are shown in Figure 3. Regardless of the sample, a dominant symmetric doublet is observed, with hyperfine parameters given in Table 2, typical for high-spin Fe^{2+} in ionic compounds of tetrahedral

Table 2. Room temperature Mössbauer results of major doublet in the Mg doped orthosilicate samples.

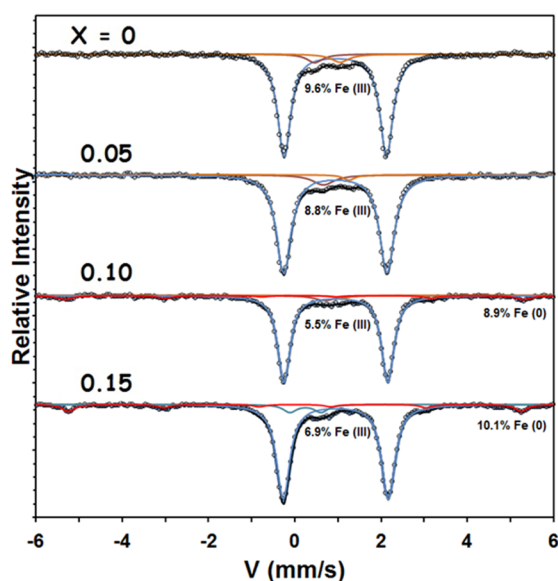| Amount of Mg doping / mol%	CS / mm s⁻¹	QS / mm s⁻¹	HWHM / mm s⁻¹	A / %
0	0.939(2)	2.374(4)	0.180(3)	90.4
5	0.940(2)	2.394(4)	0.202(3)	91.2
10	0.952(1)	2.407(4)	0.171(3)	85.7
15	0.948(2)	2.437(4)	0.187(3)	83.8

Figure 3. Room temperature Mössbauer spectra of Mg doped orthosilicate samples.

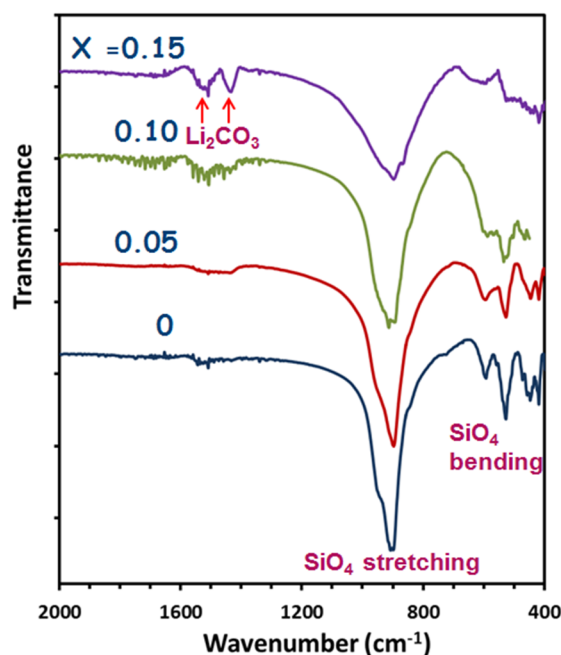**Figure 4.** FTIR spectra of Mg doped Li_2FeSiO_4 samples. Peaks at 1431 cm^{-1} and 1500 cm^{-1} are attributed to Li_2CO_3 formed at the surface.

environment. Of the different polymorphs of Li_2FeSiO_4 proposed, the isomer shift and quadrupole splitting values of both, the pristine and doped materials, match with those of the monoclinic structure $P2_1/n$.[17–21] This result is supported by the XRD and FTIR analysis. The quadrupole
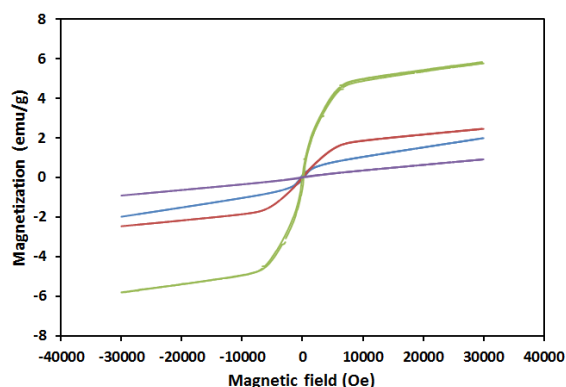

Figure 5. Room temperature magnetization curves of $Li_2Fe_{1-x}Mg_xSiO_4$, $0 \leq x \leq 0.15$.

splitting was found to increase monotonically with increasing Mg content, suggesting a diminishing distortion of the iron sites. As pointed out by Mali *et al.*,[12] the quadrupole splitting values can be correlated to the distortion of the FeO_4 tetrahedra, with a trend of larger quadrupole splitting for lesser distortion. In addition to the Fe^{2+} doublet, a small absorption area in the center of each of the Mössbauer spectrum was also observed, associated with a Fe^{3+} phase. The central resonance absorption in the Mössbauer spectra of undoped and Mg-doped samples up to 10 % (mole fraction) were fitted with two broad singlets which are attributed to nanoparticles of lithiated iron oxides,[21,22] whereas in the case of the 15 % (mole fraction) sample a doublet was used, corresponding to delithiated orthosilicate $LiFeSiO_4$.[23,24] These impurities are imperceptible or hardly detected by XRD or in the FTIR spectra. It is important to note that, disregarding the fitting model used for the Mössbauer spectra, the hyperfine parameters of the Fe^{2+} doublet remain unchanged. A small contribution from a sextet is observed for samples with equal or exceeding 10 % (mole fraction) doping metal. Data clearly show that Mg doping is accompanied by reduction of Fe^{2+} to BCC iron (saturated solid solution of magnesium in iron [25]), with a Mössbauer hyperfine field varying from 32.9 T to 32.5 T. An increase in Mg doping causes segregation of a magnetic phase. There is a monotonic increase of this magnetic phase in samples with more than 10 % (mole fraction) Mg doping, according to results that are not presented here.

FTIR spectra, shown in Figure 4, have all the attributes of Li_2FeSiO_4. The peak at 907 cm^{-1} in the undoped orthosilicate can be attributed to the stretching vibration of $(SiO_4)^{4-}$ group.[26] A slight shift of this band towards lower frequencies *i.e.* 897 cm^{-1} might be associated with changes in the local environments because of Mg doping. The shoulder band observed at around 950 cm^{-1} is due to SiO apical stretching vibrations.[27] The peaks below 600 cm^{-1}

i.e. 52 7 cm^{-1} and 594 cm^{-1} can be ascribed to the bending vibration of tetrahedra $(SiO_4)^{4-}$.[28] Peaks at 1431 cm^{-1} and 1500 cm^{-1} present in all samples and clearly seen in the 15 % (mole fraction) doped sample, point to some amount of Li_2CO_3 formed at the surface due to lithium removal from the original structure caused by oxidation in air.[15,29] The Li_2CO_3 phase is not detectable by X-ray diffraction due to its low content and crystallinity. The formation of the delithiated orthosilicate $LiFeSiO_4$ gives a hint on the nature of the Fe^{3+} detected in the X-ray and Mössbauer measurements. A salient feature of the FTIR spectra shown in Figure 4 is the increasing peak broadening with Mg doping. Infrared line broadening is frequently observed in Li_2FeSiO_4 samples.[30–32] Line broadening has been associated with cation substitutions and ordering in silicate minerals.[33] Vanadium substitution on Li_2FeSiO_4/C composites, for example, results in significant broadening of infrared lines.[34] In $Li_2Fe_{1-x}Ba_xSiO_4$ samples, this spectra profile variation is attributed to microstructure and surface morphology of different Li_2FeSiO_4 samples.[31]

Magnetization curves for $Li_2Fe_{1-x}Mg_xSiO_4$ (x = 0, 0.05, 0.10, 0.15) crystalline powders at room temperature, given in Figure 5, indicate a large contribution of a paramagnetic phase, also observed in the Mössbauer spectra as the paramagnetic Fe^{+2} and Fe^{+3} sites. No change is observed in the paramagnetic nature of the Li_2FeSiO_4 after doping with magnesium. Some soft ferromagnetic or ferrimagnetic component is present in these materials, most likely the metallic iron phase detected by both XRD and Mössbauer. This magnetic component increases with the Mg content, indicating that this atom makes unstable the Fe presence in the original monoclinic structure, and it refines also the nanostructure of this phase. The last aspect was detected by XRD which shows that the mean crystallite size decreases with increasing Mg content. As was proved by SEM measurements the particles are micrometric and agglomerated, and present a spherical shape. In accordance with the obtained crystallite size (nanometric) each particle is polycrystalline. The undoped Li_2FeSiO_4 shows a behavior typical of a paramagnetic material in agreement with the results reported by Lv *et al.*[19]

CONCLUSION

Mg doped Li_2FeSiO_4 was synthesized via a solid-state reaction. Both, pristine and doped materials consist of the monoclinic structure (space group: $P2_1/n$) as verified by Mössbauer spectroscopy, X-ray diffraction and FTIR. Some small amounts of electrochemical deleterious Fe^{3+} impurities, like lithium iron oxide or lithiated magnetite, are obtained for the undoped material. Magnesium doped materials with up to 5 % (mole fraction) Mg^{2+} retain the paramagnetic monoclinic structure and lattice parameter,

which indicates that doping agent gets into the structure of Li_2FeSiO_4 without destroying its lattice structure. A magnetic phase is segregated for samples with equal or exceeding 10 % (mole fraction) doping metal. Data clearly show that Mg doping is accompanied by reduction of Fe^{2+} to magnetic BCC iron. The SEM images have proved that Mg-doped particles form an agglomerate of small sphere-like particles with a wide particle size distribution. No clear tendency in the lattice parameters and crystallite size is observed after Mg^{2+} doping.

REFERENCES

[1] A. Nytén, A. Abonimrane, M. Armand, T. Gustafsson, J. O. Thomas, *Electrochem. Commun.* **2005**, *7*, 156.

[2] K. C. Kam, T. Gustafsson, J. O. Thomas, *Solid State Ionics* **2011**, *192*. 356.

[3] Y. Chen, Y. Zhao, X. An, J. Liu, Y. Dong, C. Ling, *Electrochim. Acta* **2009**, *54*, 5844.

[4] C. Deng, S. Zhang, S. Y. Yang, B. L. Fu, J. Ma, *J. Power Sources* **2011**, *196*, 386.

[5] B. Shao, I. Taniguchi, *J. Power Sources* **2012**, *199*, 278.

[6] Y. S. Li, X. Cheng, Z. Zhang, *J. Electrochem. Soc.* **2012**, *159*, A69.

[7] S. Zhang, C. Deng, B. L. Fu, S. Y. Yang, L. Mab, *J. Electroanal. Chem.* **2010**, *644*, 150.

[8] X. Huang, H. Chen, H. Li, Q. Yang, S. Zhou, Y. Chen, B. Liu, J. Yang, *Appl. Mech. Mater.* **2013**, *310*, 90.

[9] H. Yamashita, S. Ishihara, T. Ogami, *Pacific cement research report* **2013**, *165*, 42.

[10] A. Örnek, O Efe, *Electrochim. Acta* **2015**, *166*, 338.

[11] A. Larson, R. Von Dreele, *General Structure Analysis System (GSAS), Los Alamos National Laboratory Report. LAUR* 86-748, **2004**.

[12] G. Mali, C. Sirisopanaporn, C. Masquelier, D. Hanzel, R. Dominko, *Chem. Mater.* **2011**, *23*, 2735.

[13] C. Sirisopanaporn, C. Masquelier, P. Bruce, A. Armstrong, R. Dominko, *J. Am. Chem. Soc.* **2011**, *133*, 1263.

[14] M. Pernet, P. Strobel, B. Bonnet, P. Bordet, *Solid State Ionics* **1993**, *66*, 259.

[15] P. Zuo, T. Wang, G. Cheng, C. Du, Y. Ma, X. Cheng, G. Yin, *J. Solid State Electrochem.* **2013**, *17*, 1955.

[16] J. A. Jaén, M. Jiménez, E. Flores, A. Muñoz, J. A. Tabares, G. A. Pérez Alcázar, *Hyperfine Interact.* **2015**, *232*, 127.

[17] D. Jugović, M. Milović, V. N. Ivanovski, M. Avdeev, R. Dominko, B. Jokić, D. Uskoković, *J. Power Sources* **2014**, *265*, 75.

[18] G. Mali, C. Sirisopanaporn, C. Masquelier, D. Hanzel, R. Dominko, *Chem. Mater.* **2011**, *23*, 2735.

[19] D. Lv, W. Wen, X. Huang, J. Bai, J. Mi, S. Wu, Y. Yang, *J. Mater. Chem.* **2011**, *21*, 9506.

[20] C. Sirisopanaporn, A. Boulineau, D. Hanzel, R. Dominko, B. Budic, A. R. Armstrong, P. G. Bruce, C. Masquelier, *Inorg. Chem.* **2010**, *49*, 7446.

[21] R. Dominko, D. E. Conte, D. Hanzel, M. Gaberscek, J. Jamnik, *J. Power Sources* **2008**, *78*, 842.

[22] P. Domingues, E. Nuñez, and J. Neto, *J. Magn. Magn. Mater.* **1991**, *96*, 101.

[23] J. Fontcuberta, J. Rodríguez, M. L. Pernet, J. B. Goodenough, *J. App. Phys.* **1986**, *59*, 1918.

[24] I. K. Lee, S. J., Kim, T. Kouh, C. S. Kim, *J. Appl. Phys.* **2013**, *113*, 17E306.

[25] G. A. Dorofeev, E. P., Elsukov, A. L. Ul'yanov, *Inorg. Mater.* **2004**, *40*, 690.

[26] J. Bai, Z. Gong, D. Lv, Y. Li, H. Zou, Y. Yang, *J. Mater. Chem.* **2012**, *22*, 12128.

[27] R. L. Frost, J. M. Bouzaid, W. N. Martens, B. J. Reddy, *J. Raman Spectrosc.* **2007**, *38*, 135.

[28] S. Singh, S. Mitra, *Electrochim. Acta* **2014**, *123*, 378.

[29] C. Deng, S. Zhang, Y. Gao, B. Wu, L. Ma, Y. H. Sun, B. L. Fu, Q. Wu, F. L. Liu, *Electrochim. Acta* **2011**, *56*, 7327.

[30] R. Fu, Y. Li, H. Yang, Y. Zhang, X. Cheng, *J. Electrochem. Soc.* **2013**, *160*, A3048.

[31] C. Kim, G. W. Yoo, J. T. Son, *J. Nanosci. Nanotechnol.* **2015**, *15*, 8808.

[32] Y. Xu, W. Shen, A. Zhang, H. Liu, Z. Ma, *J. Mater. Chem. A* **2014**, *2*, 12982.

[33] T. Boffa Ballarana, *Phase Transit.* **2003**, *76*, 137.

[34] Y. Hong, Z. Ying, C. Xuan, *J. Electrochem.* **2013**, *19*, 565.